12-10-2012

# Increased normal incidence photocurrent in quantum dot infrared photodetectors

Jiayi Shao
*Purdue University, Birck Nanotechnology Center*, shao20@purdue.edu

Thomas E. Vandervelde
*Tufts University*

Ajit Barve
*University of New Mexico - Main Campus*

Andreas Stintz
*University of New Mexico - Main Campus*

Sanjay Krishna
*University of New Mexico - Main Campus*

AIP | Applied Physics Letters

# Increased normal incidence photocurrent in quantum dot infrared photodetectors

Jiayi Shao, Thomas E. Vandervelde, Ajit Barve, Andreas Stintz, and Sanjay Krishna

Citation: Appl. Phys. Lett. **101**, 241114 (2012); doi: 10.1063/1.4764905
View online: http://dx.doi.org/10.1063/1.4764905
View Table of Contents: http://apl.aip.org/resource/1/APPLAB/v101/i24
Published by the American Institute of Physics.

# Increased normal incidence photocurrent in quantum dot infrared photodetectors

Jiayi Shao,[1] Thomas E. Vandervelde,[2] Ajit Barve,[3] Andreas Stintz,[3] and Sanjay Krishna[3]
[1]*Birck Nanotechnology Center, Purdue University, 1205 W State Street, West Lafayette, Indiana 47907, USA*
[2]*Department of Electrical and Computer Engineering, Tufts University, 161 College Ave., Medford, Massachusetts 02155, USA*
[3]*Center for High Technology Materials, ECE Department, University of New Mexico, 1313 Goddard St SE, Albuquerque, New Mexico 87106, USA*

(Received 17 August 2012; accepted 16 October 2012; published online 12 December 2012)

We have increased the ratio of s-polarization (normal incidence) to p-polarization photocurrent to 50% in a quantum dot-in-a-well based infrared photodetector form the typical s-p polarization ratio about 20%. This improvement was achieved by engineering the dot geometry and the quantum confinement via post growth capping materials of the Stranski Krastanov growth mode quantum dots (QDs). The TEM images show that the height to base ratio of shape engineered QDs was increased to 8 nm/12 nm from the control sample's ratio 4 nm/17 nm. The dot geometry correlates with the polarized photocurrent measurements of the detector. © *2012 American Institute of Physics*. [http://dx.doi.org/10.1063/1.4764905]

In the past decade, quantum dot infrared photodetectors (QDIP) have been a subject of active research. There has been significant progress in the performance of these detectors in the past five years as outlined in this review paper.[1] In particular, dots-in-a-well (DWELL) detectors, in which quantum dots are placed in InGaAs/GaAs/AlGaAs quantum wells, have demonstrated low dark currents and multispectral imagery.[2–8] Large format megapixel images, two color detectors, and bias tunable detectors have been demonstrated.[8–11] Theoretically, QDIPs offer several advantages, including lower dark current, higher operating temperature, higher photoresponsivity, normal incidence detection, and improved radiation hardness.[2–11] Most of these attributes arise from the 0-D confinement that is expected to increase the photon-excited carrier lifetime by reducing optical phonon scattering via the "phonon bottleneck" mechanism.[12,13]

Although self-assembled QDs have performed impressively in a variety of electronic and optoelectronic devices, their full potential has not been achieved. This is mostly due to the fact that the epitaxially grown quantum dots tend to be "pancake shaped" due to the flattening of the dots via interface intermixing during the growth of the capping layer. Both the flattened shape and intermixed interface of QDs lead to the weakness of discrete quantum mechanical confinement[14,15] by modifying the density of states and thereby suppress interesting phenomenon like the "phonon bottleneck." Moreover, the s-polarization (normal incidence) absorption in quantum dot detectors is a factor of five (20%) lower than the p-polarization response.[16] Thus in normal incidence quantum dot imagery without gratings, 80% of the signal is not utilized. In this paper, we report the shape engineered QDs with reduced intermixing between the dots and the capping layers. This has enabled us to evolve from "pancake shaped" dots (shown schematically in Fig. 1(a)) with a height of 4 nm and a base of 17 nm to "cone shaped" dots (shown schematically in Fig. 1(b)) with height of 8 nm and base of 12 nm, as obtained from cross sectional transmission electron microscopy (TEM). The change in the aspect ratio of the dot was confirmed by polarization dependent photocurrent measurements, in which the s-p polarization ratio was increased from 20% to 50% in the control sample. This represents a significant step in obtaining strongly 0D confined quantum dots that can be used for a wide variety of applications.

The key to shape engineering revolves around the control of the diffusion processes involved in the intermixing between the QDs and the capping material. This diffusion can be controlled through several means: interfacial-strain engineering, mechanical diffusion barrier, and chemical diffusion retardant, and/or deposition kinetics. Initial results verify that interfaces with less strain should intermix less, due to decreased availability of energy drives less diffusion.[14,15,17] So InAs-based compounds were considered. Certain materials (e.g., Al) can act as both mechanical diffusion barrier and chemical diffusion retardant for the indium in our InAs dots. By controlling the temperature and rate of deposition, the deposition kinetics can be controlled. Furthermore one should be able to mitigate the enhanced diffusion generated by the increased interfacial energy. To try to find a balance between these energies and follow previous results, we employed InAlGaAs as the compounds in our study.[16]

Two samples for this study were grown using VG80 solid-source molecular beam epitaxy (MBE) system with a cracked $As_2$ source. A conventional DWELL detector (sample A) was used as a control sample. Sample A has 2.8 ML InAs quantum dots embedded in 3 nm $In_{0.15}Ga_{0.85}As$ lower quantum well bed and 2.5 nm cap layer of $In_{0.15}Ga_{0.85}As$ quantum well. The DWELL structure is followed with a 50 nm $Al_{0.08}Ga_{0.92}As$ barrier, and the active region was repeated 20 times. A shape engineered QDs sample (sample B) was also grown. In sample B, the 2.8 ML InAs quantum dots were grown on a 4 nm $In_{0.15}Al_{0.1}Ga_{0.75}As$ lower quantum well with 1 nm $In_{0.15}Ga_{0.85}As$ strain bed, then the QDs were capped with a 6.8 nm $In_{0.15}Al_{0.1}Ga_{0.75}As$ upper quantum well to minimize intermixing. The barrier layer consisted of 50 nm $Al_{0.3}Ga_{0.7}As$, and this active layer was

 

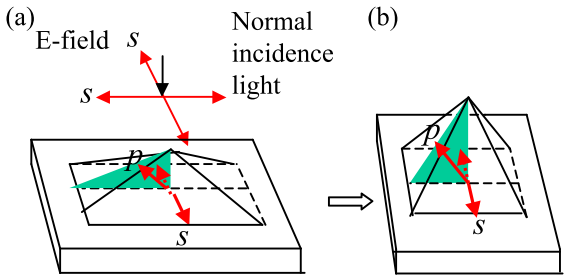


FIG. 1. (a) Flattened QDs in epitaxial growth via intermixing during subsequent growth. (b) Engineered QDs with decreased base size and increased height.

repeated 12 times. Both samples had a 500 nm $n^+$GaAs bottom contact layer and 200 nm $n^+$GaAs top contact layer. Standard processing techniques were then applied for the device fabrication. 450 $\mu$m diameter circular mesa with GeAu top and bottom contact rings were formed to allow normal incidence measurement from the top window.

Fig. 2(a) is a high-resolution STEM image of the QD in the reference sample A. The bright area shows the indium atom distribution. It reveals that the dot is confined to the top half of the quantum well, and there are obvious indium diffusion between the interface of the dot and the capping material. The QD is pancake shaped with a base width of ~17 nm and height of ~4 nm, and the height to base aspect ratio is 0.23. Fig. 2(b) is a high-resolution TEM image of the shape engineered QD in sample B. The dark area indicates the high strain area. It reveals that the dot is confined to the top half of the well and the QD cross section in the [110] azimuth is triangle-like with a base width of ~12 nm and height of ~8 nm, respectively. The height to base aspect ratio is 0.67. The edge between the dot and the capping material is clear and no obvious diffusion is observed. Thus the engineered QDs design prevents the diffusion processes involved in the intermixing between the QDs and the capping material, reduces the dot base width, increases the dot height, and improves the 0-D quantum confinement.

For polarization dependent infrared spectral response measurements, the experimental setup schematic and the front and back view of the 45° leadless chip carrier (LCC) are shown in Fig. 3(a). The processed devices were polished with 45° facet geometry, mounted on the 45° facet holder, and wire-bonded on the pins of the LCC. The polarization of the incoming infrared beam was either *s* polarized in which case the E-field is in the growth plane or *p* polarized in which

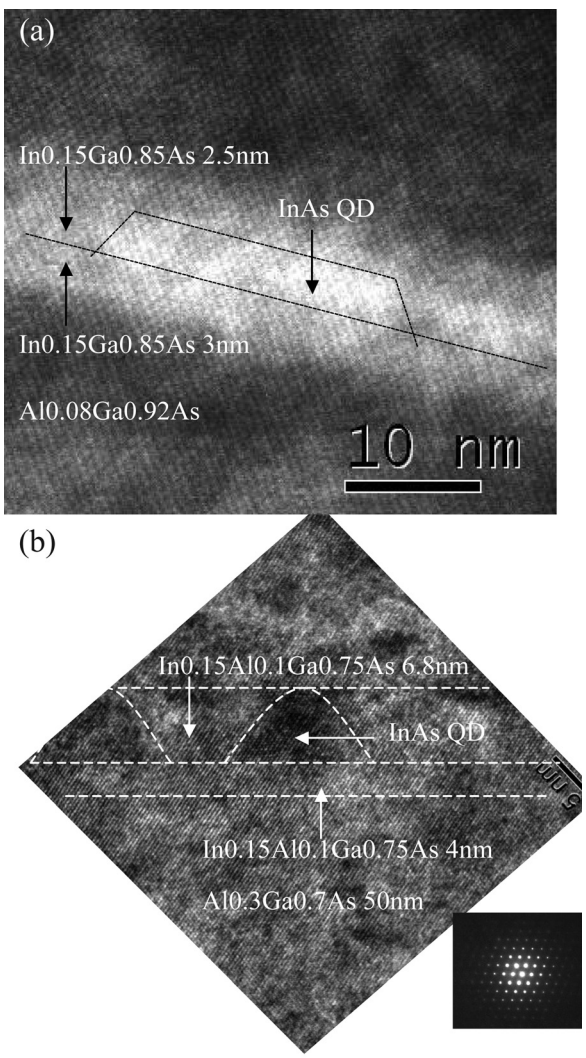


FIG. 2. (a) The high resolution STEM image of the QD in the reference sample A. (b) The high resolution TEM image of the engineered QD in the sample B.

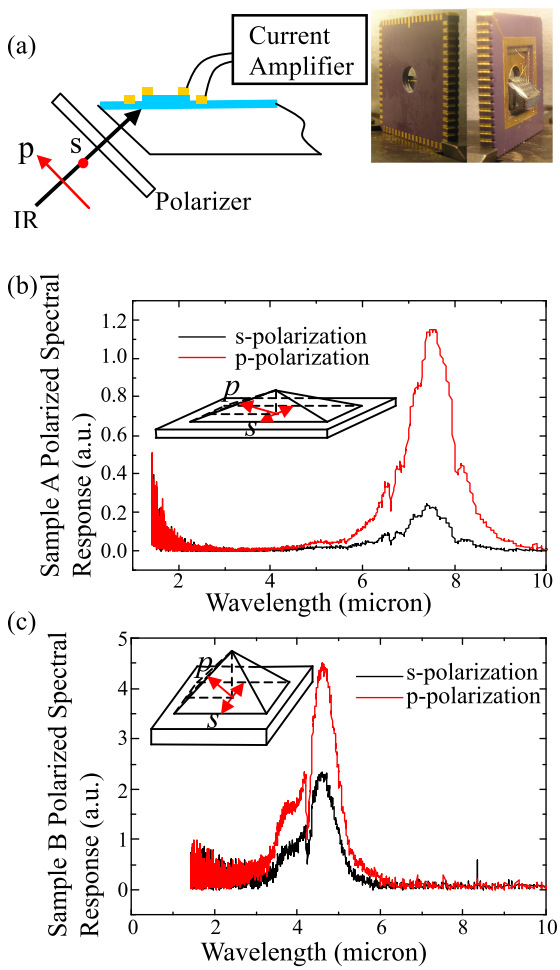


FIG. 3. (a) The experimental setup schematic of the polarized spectral response measurements, and front and back view of the 45° facet leadless chip carrier. (b) The s and p polarized infrared spectral response of reference QD sample A measured at 77 K (−4.5 V). (c) The s and p polarized infrared spectral response of engineered QD sample B measured at 77 K (+13 V).

case the E-field has a 50% component along the growth direction as shown in insets of Figs. 3(b) and 3(c).[18–20] Fig. 3(b) shows s and p polarization dependent spectral response of sample A at 77 K ($V_b = -4.5$ V). It indicates that the ratio of the s/p infrared polarized photocurrent of the reference sample is less then 20%. The in-plane quantum confinement and in-plane infrared absorption are much lower than the vertical direction. For the normal incidence (s-polarization) without gratings, more than 80% of signal is not utilized.

The results measured at 77 K ($V_b = +13$ V) in Fig. 3(c) indicate that the ratio of the *s*/*p* polarization dependent spectral response of the sample B increases to 50%, respectively. This is the highest *s*/*p* polarization ratio observed in a spectral response measurement. A strong spectral response describes not only the high material quality of QDs, such as low defect density and low trap center density, but also the strong discrete quantum confinement and less intermixing and leakage path of the interface between QDs and capping materials.[14–17] For conventional Stranski-Krastanov QDs, the *s* polarized absorption is always less then the *p* polarized absorption,[16] but the improved *s*/*p* ratio as 50% indicates the in-plane quantum confinement and in-plane infrared absorption are dramatically improved than the vertical direction. This also corroborates the results of the TEM images. The behaving of engineered QDs is more close to the idea 0-D quantum confinement.

In conclusion, we have demonstrated a shape engineered QD detector with increased height to base ratio as 0.67 compared to a conventional QD detector as 0.23. The change in the QDs geometry aspect ratio was observed using TEM. A significant increasing in the *s*/*p* polarization ratio was measured using the polarization dependent photocurrent. We believe that the use of an InAlGaAs cap prevents the flattening of QDs by reducing the diffusion gradient. This is expected to increase the carrier relaxation time by providing strong 0D quantum mechanical confinement.

The authors would like to acknowledge support from AFRL Contract and AFOSR Contract.

[1]A. V. Barve, S. J. Lee, S. K. Noh, and S. Krishna, Laser Photon. Rev. **4**(6), 738–750 (2010).
[2]S. Krishna, J. Phys. D **38**, 2142 (2005).
[3]E. T. Kim, A. Madhukar, Z. Ye, and J. C. Campbell, Appl. Phys. Lett. **84**, 3277 (2004).
[4]J. Phillips, J. Appl. Phys. **91**, 4590 (2002).
[5]S. Tsao, H. Lim, W. Zhang, and M. Razeghi, Appl. Phys. Lett. **90**, 201109 (2007).
[6]G. Jolley, L. Fu, H. H. Tan, and C. Jagadish, Appl. Phys. Lett. **92**(19), 193507 (2008).
[7]P. Martyniuk, S. Krishna, and A. Rogalski, J. Appl. Phys. **104**(3), 034314 (2008).
[8]M. N. Abedin, T. F. Refaat, J. Zawodny, S. P. Sandford, U. N. Singh, S. Bandra, S. D. Gunapala, I. Bhat, and N. P. Barnes, Proc. SPIE **5152**, 279–288 (2003).
[9]G. Ariyawansa, S. Matsik, A. Perera, X. Su, and P. Bhattacharya, 2007 IEEE Sens. pp. 503–506.
[10]S. D. Gunapala, S. V. Bandara, J. K. Liu, J. M. Mumolo, D. Z. Ting, C. J. Hill, J. Nguyen, B. Simolon, J. Woolaway, S. C. Wang, L. Wiping, P. D. LeVan, and M. Z. Tidrow, J. Quant. Elect. **46**, 285–293 (2010).
[11]Vines, P. Tan, C. H. David, J. P. R. Attaluri, R. S. Vandervelde, T. E. Krishna, S. Jang, and W. Y. Hayat, in IEEE LEOS Annual Meeting Conference Proceedings, 4-8 October 2009, pp. 166–167.
[12]J. Urayama, T. B. Norris, J. Singh, and P. Bhattacharya, Phys. Rev. Lett. **86**(21), 4930–4933 (2001).
[13]P. Aivaliotis, S. Menzel, E. A. Zibik, J. W. Cockburn, L. R. Wilson, and M. Hopkinson, Appl. Phys. Lett. **91**(25), 253502 (2007).
[14]J. M. García, G. Medeiros-Ribeiro, K. Schmidt, T. Ngo, J. L. Feng, A. Lorke, J. Kotthaus, and P. M. Petroff, Appl. Phys. Lett. **71**, 2014 (1997).
[15]J. Shao, T. Vandervelde, W. Jang, A. Stintz, and S. Krishna, IEEE Trans. Nanotechnol. **10**(5), 1010–1014 (2011).
[16]H. C. Liu, Opto-Electron. Rev. **11**(1), 1–5 (2003).
[17]A. M. Sanchez, R. Beanland, N. F. Hasbullah, M. Hopkinson, and J. P. R. David, J. Appl. Phys. **106**, 024502 (2009).
[18]C.-C. Tseng, S.-T. Chou, Y.-H. Chen, C.-N. Chen, W.-H. Lin, T.-H. Chung, S.-Y. Lin, P.-C. Chiu, J.-I. Chyi, and M.-C. Wu, IEEE Photon. Technol. Lett. **20**(14), 1240–1242 (2008).
[19]S. D. Gunapala, S. V. Bandara, C. J. Hill, D. Z. Ting, J. K. Liu, S. B. Rafol, E. R. Blazejewski, J. M. Mumolo, S. A. Keo, S. Krishna, Y.-C. Chang, and C. A. Shott, IEEE J. Quantum Electron. **43**(3), 230–237 (2007).
[20]G. Ariyawansa, P. V. V. Jayaweera, A. G. U. Perera, S. G. Matsik, M. Buchanan, Z. R. Wasilewski, and H. C. Liu, Opt. Lett. **34**, 2036 (2009).